Mixed-ligand, radical, gold bis(dithiolene) complexes: from single-component conductors to controllable NIR-II absorbers†

Haia Kharraz,[a] Pere Alemany,[b] Enric Canadell,*[c,d] Yann Le Gal,[a] Thierry Roisnel,[a] Hengbo Cui,[e] Kee Hoon Kim,[e] Marc Fourmigué*[a] and Dominique Lorcy*[a]

[a] *UnivRennes, CNRS, ISCR (Institut des Sciences Chimiques de Rennes), 35042 Rennes, France. E-mail: marc.fourmigue@univ-rennes.fr, dominique.lorcy@univ-rennes.fr*

[b] *Departament de Ciència de Materials i Química Física and Institut de QuímicaTeòrica i Computacional (IQTCUB), Universitat de Barcelona, Martí i Franquès 1, 08028 Barcelona, Spain*

[c] *Institut de Ciencia de Materials de Barcelona, ICMAB-CSIC, Campus de la UAB, 08193 Bellaterra, Spain. E-mail : canadell@icmab.es*

[d] *Royal Academy of Sciences and Arts of Barcelona, Chemistry Section, La Rambla 115, 08002 Barcelona, Spain*

[e] *Institute of Applied Physics, Department of Physics and Astronomy, Seoul National University, Seoul 08826, Korea*

SUPPLEMENTARY INFORMATION

General

Chemicals and materials from commercial sources were used without further purification. All the reactions were performed under an argon atmosphere. NMR spectra were obtained in $CDCl_3$ unless indicated otherwise. Chemical shifts are reported in ppm, ^1H NMR spectra were referenced to residual $CHCl_3$ (7.26 ppm) and ^{13}C NMR spectra were referenced to $CHCl_3$ (77.2 ppm). Melting points were measured on a Kofler hot-stage apparatus and are uncorrected. Mass spectra were recorded by the Centre Régional de Mesures Physiques de l'Ouest, Rennes. Methanol, acetonitrile and dichloromethane were dried using Inert pure solvent column device. Cyclic voltammetry has been performed in a three-electrode cell equipped with a platinum disk working electrode and a glass carbon as counter-electrode. CVs were carried out on a 10^{-3} M solution of complex in CH_2Cl_2 with 0.1 M $[Bu_4N][PF_6]$. Potentials were measured *versus* Saturated Calomel Electrode (SCE). Under these experimental conditions, the Fc^+/Fc couple is observed at +0.39 V *vs*. SCE. The spectroelectrochemical setup was performed in CH_2Cl_2-$[NBu_4][PF_6]$ 0.2 M using a Pt grid as the working electrode, a Pt wire as the counter electrode and SCE reference electrode. A Shimadzu 3600 plus spectrophotometer was used to record the UV-vis-NIR spectra. The starting products $[Bu_4N][Au(bdt)Cl_2]$ **3** and Et-thiazdt$(CH_2CH_2CN)_2$ **4** were prepared as previously described.[1,2] 2,3-Pyrazinedithiol was prepared from 2,3-dichloropyrazine.[3]

Syntheses

Synthesis of [Bu_4N][Au(bdt)(Et-thiazdt)] ***1***. Under an inert atmosphere, 1,8-diazabicyclo[5.4.0]undec-7-ene (DBU) (0.45 ml, 3 mmol) was added to a solution of the gold complex **3** (0.1 mg, 0.15 mmol) and the protected dithiolene ligand **4** (0.47 g, 0.15 mmol) in 10 ml of dried CH_2Cl_2. The addition of DBU generates a rapid change of color from dark to light brown solution. After stirring for 21 h at room temperature, water was added to the reaction mixture, and the organic phase was washed with water several times and dried over $MgSO_4$. The solvent was removed under vacuum and acetonitrile was added to precipitate insoluble material, the precipitate was filtered off and the filtrate was concentrated. The crude product was dissolved in 1 ml CH_2Cl_2 and the product was precipitated by the addition of diethyl ether. The complex was recrystallized in MeOH to afford salt **1** as brown crystals in 66% yield. M. p. 98-100°C; ^1H NMR (300 MHz, CD_3CN) δ 7.18 – 7.06 (m, 2H), 6.97 – 6.85 (m, 2H), 4.16 (q, J = 7.1 Hz, 2H), 3.13 – 3.01 (m, 9H), 1.58 (ddt, J = 15.1, 11.9, 7.0 Hz, 9H), 1.44 – 1.21 (m, 12H), 0.96 (t, J = 7.3 Hz, 12H); ^{13}C NMR (75 MHz, CD_3CN) δ 191.2, 141.7, 141.5, 128.4, 128.3,

124.9, 59.3, 43.7, 24.3, 20.3, 13.7, 12.9; UV-vis (CH_3CN) λ_{abs} [nm] (ε [M^{-1} cm^{-1}]): 286 (23 500), 340 (14 000), 384 (9 600); Elem. Anal. Calcd for $C_{27}H_{45}AuN_2S_6$: C, 41.21; H, 5.76; N3.56; S, 24.44. Found: C, 41.31; H, 5.39; N, 3.65; S, 23.61.

Synthesis of 2,2-dibutyl-[1,3,2]dithiastannolo[4,5-b]pyrazine ***5***. To an ethanol solution (5 ml) containing 2,3-pyrazinedithiol (144 mg, 1 mmol) was added a 0.1M KOH solution in ethanol (10 ml). Color changes from yellow to brown upon stirring for 15 min. A solution of Bu_2SnCl_2 (303 mg, 1 mmol) in 50 ml of distilled water was added to the mixture, further stirred for 30 min at room temperature. A yellow precipitate was filtered off and washed with water, and then pentane to afford **5** as a yellow powder in 50% yield. M. p. 136°C ; ^{1}H NMR (300 MHz) δ 7.94 (s, 2H), 2.17 (s, 1H), 1.75 (t, *J* = 5.2 Hz, 11H), 1.40 (q, *J* = 7.3 Hz, 7H), 0.99 – 0.86 (m, 11H); ^{13}C NMR (75 MHz) δ 137.5, 89.8, 27.8, 26.7, 22.3, 13.6; HRMS (ASAP) calcd for $[M+H]^+$: 377.01627, found :377.0167.

Synthesis of [Bu₄N][Au(pzdt)Cl₂] ***6***. To a solution of Bu_4NCl (236 mg, 0.85 mmol) in dry CH_2Cl_2 (20ml), $KAuCl_4$ (322 mg, 0.85 mmol) was added. The reaction mixture was stirred for 30 min at room temperature under an inert atmosphere. A solution of (pzdt)$SnBu_2$ **5** (320 mg, 0.85 mmol) in 20 ml dried CH_2Cl_2 is added and the solution turned green. After refluxing the mixture for 48 hr, insoluble material was filtered off from the green cooled solution, and the filtrate was evaporated. The resulting solid was dissolved in 10 ml CH_2Cl_2, and 100 ml of ether was added. The resultant precipitate was washed by MeOH and collected by filtration to give **6** as green crystals by 80% yield. Mp 135°C. ^{1}H NMR (300 MHz) δ 8.02 (s, 2H), 3.29 – 3.18 (m, 8H), 1.75 – 1.58 (m, 8H), 1.45 (h, *J* = 7.3 Hz, 8H), 1.00 (t, *J* = 7.3 Hz, 12H);^{13}C NMR (75 MHz) δ 157.4, 137.0, 59.3, 24.3, 19.9, 13.8; Elem. Anal. Calcd for $C_{20}H_{38}AuCl_2N_3S_2(CH_2Cl_2)_{0.25}$: C, 36.10; H, 5.76; N, 6.24; S, 9.52. Found: C, 36.06; H, 6.03; N, 5.70; S, 9.30.

Synthesis of [Bu₄N][Au(pzdt)(Et-thiazdt)] ***2***. Under an inert atmosphere, 1,8-diazabicyclo[5.4.0]undec-7-ene (DBU) (0.58 ml, 3.78 mmol) was added to a solution of the gold complex **6** (120mg, 0.18mmol) and the protected dithiolene ligand **4** (58 mg, 0.18 mmol) in 10 ml of dried CH_2Cl_2. The addition of DBU generates a rapid change of color from dark to light brown. After stirring for 21 h at room temperature, water was added to the reaction mixture and the organic phase was washed with water several times and dried over $MgSO_4$. The solvent was removed under vacuum and acetonitrile was added to precipitate insoluble material, the

precipitate was filtered off and the filtrate was concentrated. The crude was dissolved in 1 ml CH_2Cl_2 and the product was precipitated by the addition of diethyl ether. The complex was recrystallized in MeOH to afford complex **2** as brown crystals in 42% yield. Mp 133°C. ^{1}H NMR (300 MHz) δ 8.03 – 7.94 (m, 2H), 4.26 (q, *J* = 7.1 Hz, 2H), 3.20 – 3.09 (m, 8H), 1.58 (t, *J* = 12.3 Hz, 8H), 1.38 (h, *J* = 7.4 Hz, 11H), 0.98 (t, *J* = 7.3 Hz, 12H); ^{13}C NMR (75 MHz, CD_2Cl_2) δ 190.7, 158.6, 136.8, 134.2, 113.2, 59.4, 43.2, 24.3, 20.1, 13.7, 12.9; UV-vis (CH_3CN) λ_{abs} [nm] (ε [M^{-1} cm^{-1}]): 281 (26 400), 348 (22 400), 378 (18 500); HRMS (ESI): calcd. for A^-($C_9H_7N_3S_6Au$): 545.86354. Found: 545.8634; Elem. Anal. Calcd. for $C_{25}H_{43}N_4AuS_6$: C, 38.06; H, 5.49; N, 7.10; S, 24.38. Found: C, 38.12; H, 5.55; N, 7.19; S, 24.70.

Electrocrystallization: Crystals of [Au(bdt)(Et-thiazdt)]$^\bullet$ **1'** were prepared electrochemically using a standard U-shaped cell equipped with Pt electrodes (1 cm length ×1 mm diameter) under inert atmosphere. An acetonitrile solution (12 mL) of the monoanionic complex **1** (5 mg) and the supporting electrolyte Et_4NPF_6 (300 mg) was placed in the U-shaped cell. A constant current intensity was adjusted to 1 μA for 3 days between the electrodes. Black plate-like crystals suitable for X-ray diffraction studies were collected at the anode and washed with CH_3CN. Under the same conditions, electrocrystallization of **2** afforded an amorphous black material (Figure S2).

Crystallography. Single-crystal diffraction data were collected on D8 VENTURE Bruker-AXS diffractometer with Mo–Kα radiation (λ = 0.71073 Å) for all compounds. The structures were solved by a dual-space algorithm using the SHELXT program,[4] and then refined with full-matrix least-squares methods based on F^2 (SHELXL-97).[5] All non-hydrogen atoms were refined with anisotropic atomic displacement parameters. H atoms were finally included in their calculated positions. Details are given in Table S5.

Computational Details. The DFT calculations for isolated molecular systems were carried out according to the prescription of Kaupp *et al.*[6] for the study of organic mixed-valence compounds. We refer the reader to this work for an excellent and very detailed discussion of the warnings and requirements for the application of DFT methods to mixed valence molecules.

Since we are interested in obtaining a qualitative description of the intrinsic preference for localized *vs.* delocalized nature of the ground state of metal dithiolenes, we have disregarded environmental effects. The D95(d,p) Dunning/Huzinaga full double zeta basis set with polarization functions[7] was used for all atoms except for Au that has been described by the SDD basis set with Stuttgart/Dresden effective core potentials.[8]

The first-principles calculations for the solid were carried out using a numeric atomic orbitals density functional theory (DFT) approach[9,10] developed for efficient calculations in large systems and implemented in the SIESTA code.[11] We used the generalized gradient approximation (GGA) to DFT and, in particular, the functional of Perdew, Burke, and Ernzerhof.[12] To study the relative energies of states with localized electrons, spin polarized band calculations for appropriate supercells have been undertaken. All calculations included a Hubbard correction term $U_{\text{eff}} = U - J = 6.0$ eV for the S 3*p* states.[13] In previous work,[14] we have found that this *U* term on the chalcogen atoms is needed for appropriately describing the electronic structure of molecular conductors where accurate experimental information on the bandwidth and charge transfer is available. Only the valence electrons are considered in the calculation, with the core being replaced by norm-conserving scalar relativistic pseudopotentials[15] factorized in the Kleinman–Bylander form.[16] We have used a split-valence double-ζ basis set including polarization orbitals with an energy shift of 10 meV[17] for S, C, N and H atoms. For gold atoms, we have used a split-valence basis set of double-ξ plus polarization quality, where the 5*d* electrons of Au were treated also as valence electrons. The basis functions used for Au have been optimized in order to reproduce the geometry and the bulk modulus for the ccp crystal structure of metallic gold.[18] The energy cutoff of the real space integration mesh was 300 Ry. The Brillouin zone was sampled using grids[19] of (10×7×3) and (10×3×3) *k*-points for the calculations with single and double cells along the transverse direction. The crystal structure at 150 K was used for the computations.

The intermolecular interaction energies were evaluated by means of extended Hückel type[20] calculations with a modified Wolfsberg-Helmholtz formula to calculate the non-diagonal $H_{\mu\nu}$ values.[21] All valence electrons were considered in the calculations and the basis set consisted of Slater-type orbitals of double-ζ quality for Au 5d, and of single-ζ quality for Au 6s and 6p, C and N 2s and 2p, S 3s and 3p and H 1s. The ionization potentials, contraction coefficients and exponents were taken from previous work.[22]

Single Crystal Resistivity Measurements:

The standard four-probe DC measurements were performed for compound **1'** by using a diamond anvil cell (DAC) using the same technique as described in Ref. 23. A rectangular shape of single crystals sample 1 ($0.14 \times 0.03 \times 0.02$ mm^3) and Sample 2 ($0.11 \times 0.04 \times 0.02$ mm^3) were used for ambient pressure and high-pressure measurements up to 8.3 GPa for sample1 and 18.1 GPa for sample 2 ($0.11 \times 0.04 \times 0.02$ mm^3). The crystal was attached by four gold wires (10 or 5μm) with gold paint. Daphne Oil 7373 was used as the pressure-transmitting medium. We used the diamond with culet size of 0.7 mm (0.56 mm) and tension-annealed stainless still SUS301 (Inconel 625) for sample 1 (sample 2). The pressure was determined by the shift of the ruby fluorescence R1 lines at room temperature. The Cryocooler helium compressor system (Sumitomo Heavy Industries, Ltd.) was used for cooling DAC with cooling rate of 1.0 K/min. The KEITHLEY 224 Programmable current source and 182 Sensitive digital voltmeter were used for all measurements.

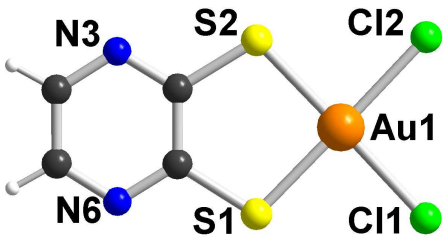

Fig. S1 Molecular structure of $[Au(pzdt)Cl_2]^-$ moiety in $[Bu_4N^+][Au(pzdt)Cl_2^-]$ **6**.

Table S1 Comparison of averaged bond lengths (in Å) within AuS_2C_2 metallacycles in **2** and the two reference symmetric complexes $[Au(pzdt)_2]^-$ and $[Au(Et\text{-}thiazdt)_2]^-$.

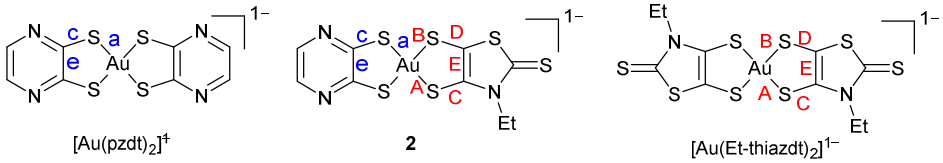

	$[Au(pzdt)_2]^{-1}$ [a]	**2**	$[Au(Et\text{-}thiazdt)_2]^{-1}$ [b]
a	2.313(3)	2.306(3)	
c	1.750(4)	1.751(4)	
e	1.409(5)	1.414(5)	
A		2.313(4)	2.329(2)
B		2.336(2)	2.332(2)
C		1.742(3)	1.760(6)
D		1.747(3)	1.744(6)
E		1.348(5)	1.332(8)

[a] As PPN salt, from Ref. 24 [b] As Et_4N^+ salt, from Ref. 25

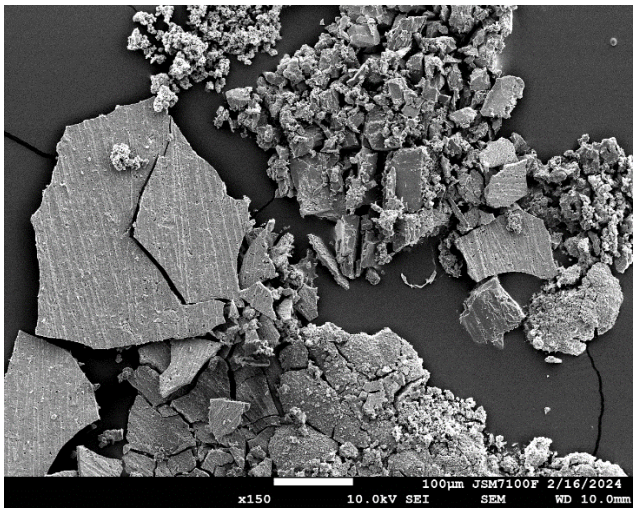

Fig. S2 SEM image of the product obtained from the electrocrystallization of **2**.

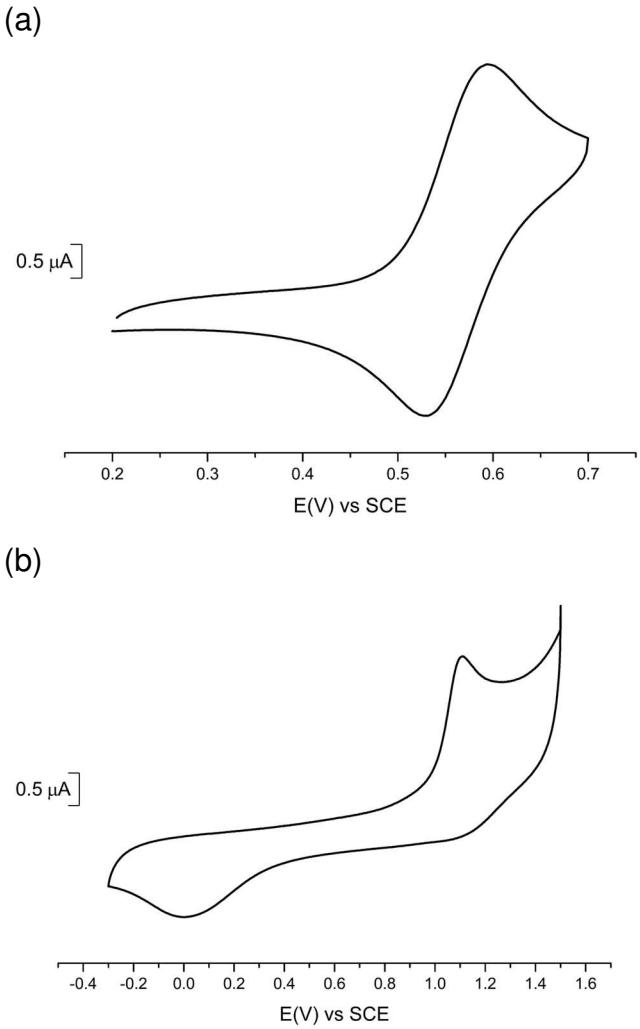

Fig. S3 Cyclic voltammetry of (a) $[Au(pzdt)(Et\text{-}thiazdt)]^{-1}$ and (b) $[Au(pzdt)_2]^{-1}$ performed in 0.1 M Bu_4NPF_6 in CH_2Cl_2 at 100 mV/s scan rate.

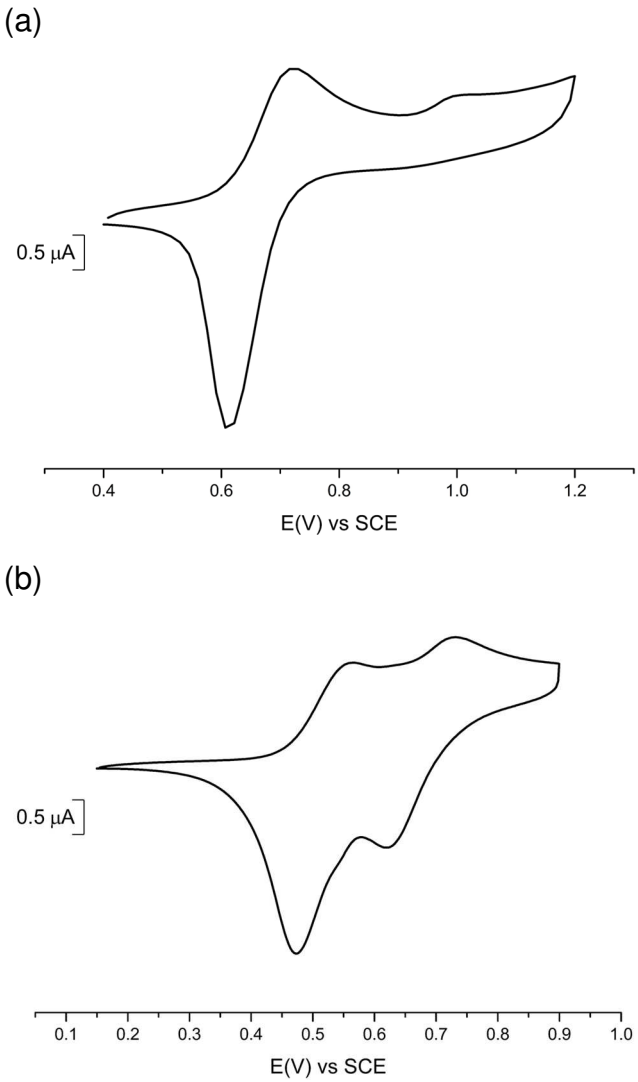

Fig. S4 Cyclic voltammetry of (a) $[Au(bdt)_2]^{-1}$ and (b) $[Au(Et\text{-}thiazdt)_2]^{-1}$ performed in 0.1 M Bu_4NPF_6 in CH_2Cl_2 at 100 mV/s scan rate.

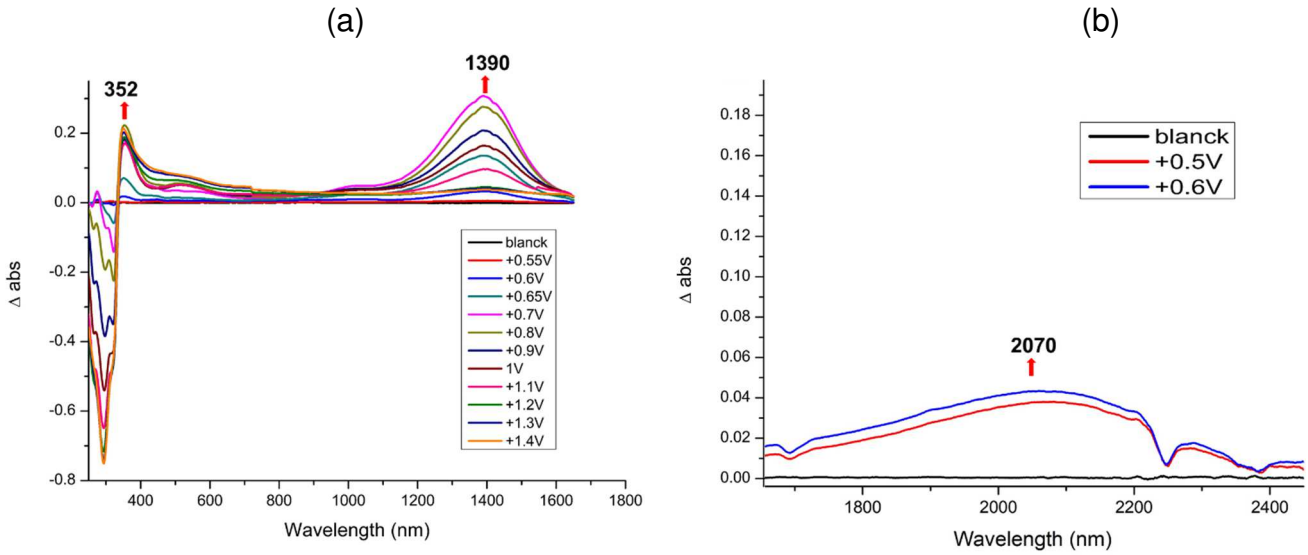

Fig. S5 Differential UV-vis-NIR absorption spectra upon incremental oxidation of (a) $[Au(bdt)_2]^{-1}$ and (b) $[Au(Et\text{-}thiazdt)_2]^{-1}$, performed in CH_2Cl_2 with Bu_4NPF_6 0.2 M. Potentials in *V vs*. SCE

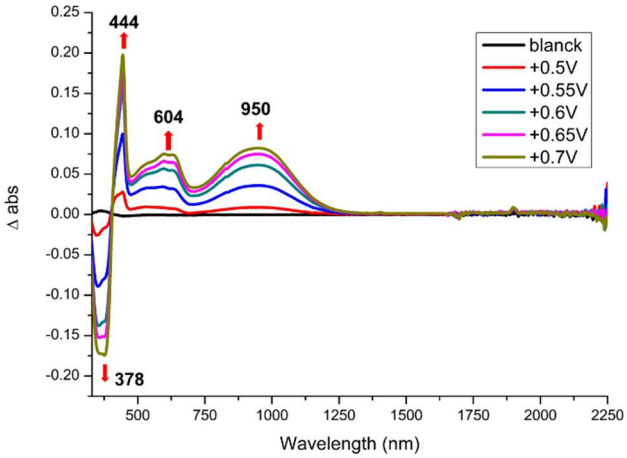

Fig. S6 Differential UV-vis-NIR absorption spectra upon incremental oxidation of [Au(pzdt)(Et-thiazdt)]$^-$ **2** into **2'**, performed in CH_2Cl_2 with Bu_4NPF_6 0.2 M. Potentials in *V vs*. SCE

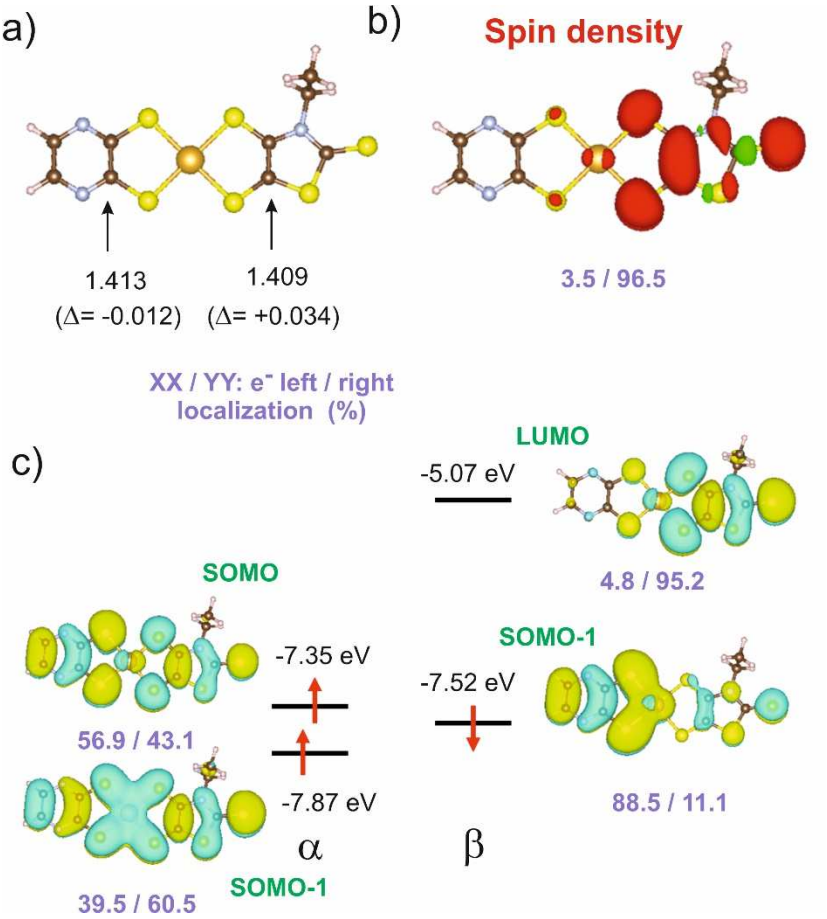

Fig. S7 [Au(pzdt)(Et-thiazdt)]• complex **2'**: (a) C=C optimized bond lengths, (b) spin density, and (c) spin-orbitals around the SOMO. The pairs of violet numbers indicate the left/right distribution (%) of the spin density in (b) or the electron distribution in a given spin-orbital in (c). In (a) the values in parenthesis are the bond length changes with respect to the corresponding symmetric complexes.

Table S2 C=C distances (Å) and first significant low energy transition (SOMO–1 → LUMO) (eV) calculated for [Au(pzdt)(Et-thiazdt)]• **2'** and the symmetric complexes.

Complex	SOMO–1→LUMO (eV)	C=C (Å)
[Au(pzdt)(Et-thiazdt)]• 2'	1.52 eV	1.413 Å (dt_A) 1.409 Å (dt_D)
[Au(pzdt)$_2$]•	0.73 eV	1.425 Å
[Au(Et-thiazdt)$_2$]•	0.45 eV	1.375 Å

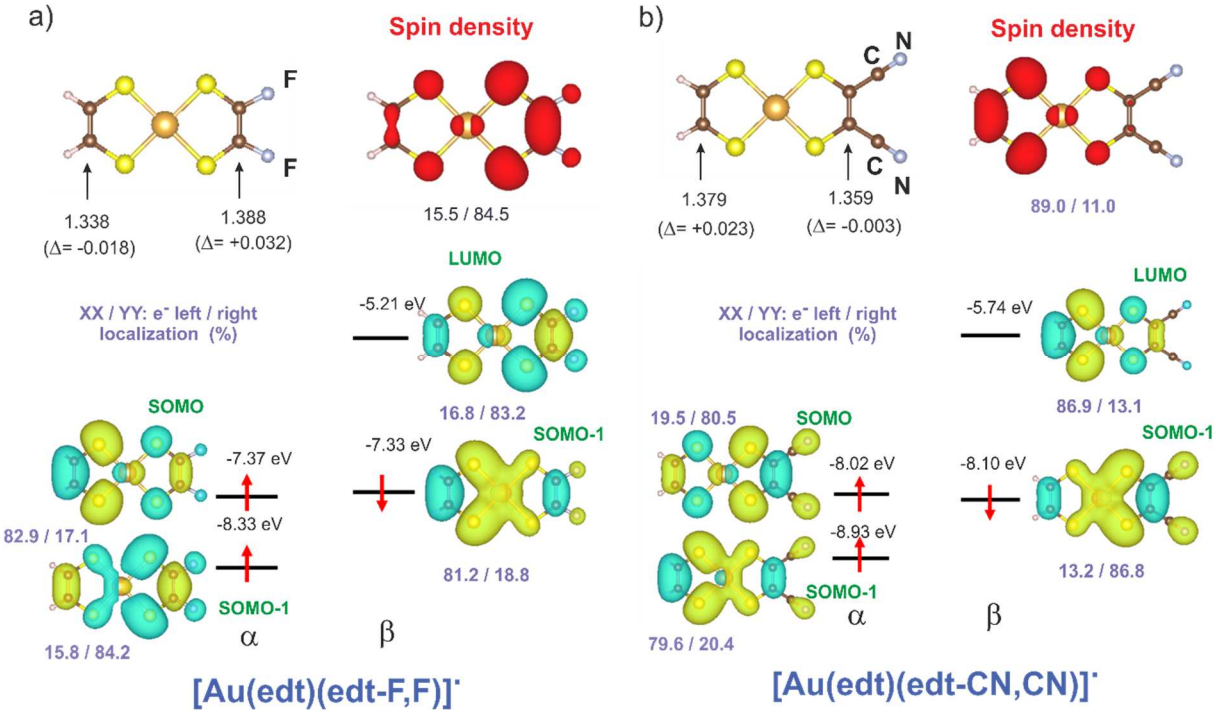

Fig. S8 Results for two [Au(edt)(edt-R,R)]• (R = F, CN) model complexes illustrating that the spin density is mostly associated with the dt_D/longer C=C side whereas the SOMO is polarized in the opposite way. For details, see captions for Figures 4 and 5.

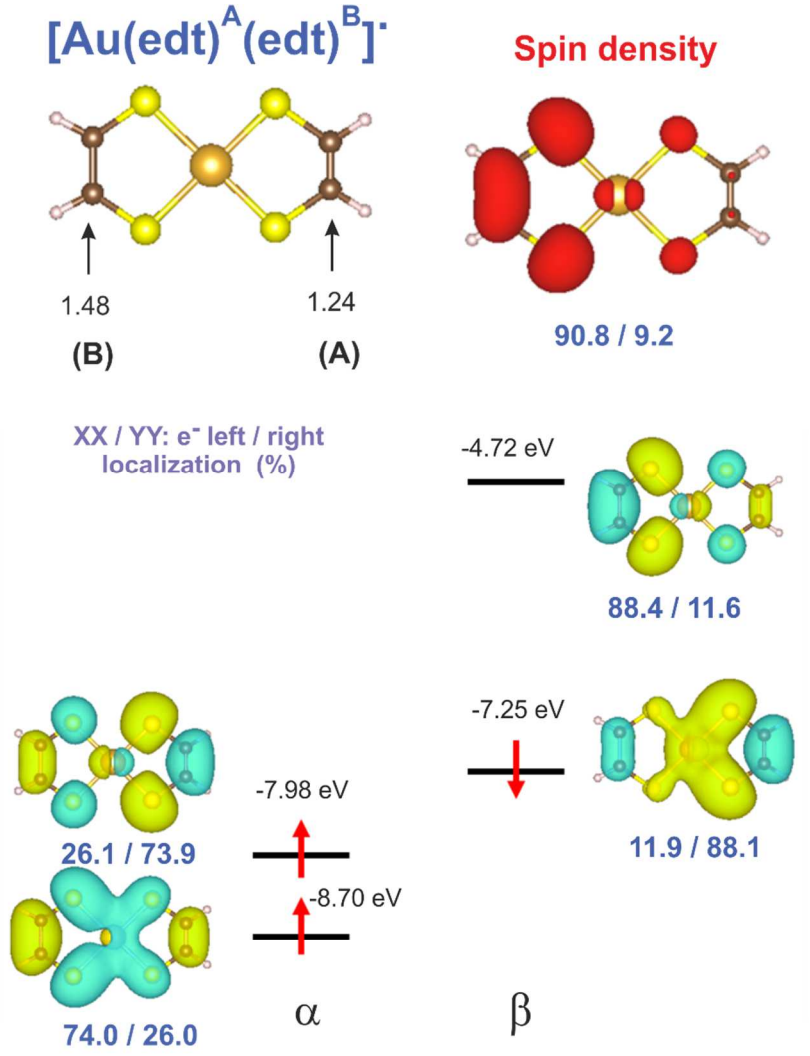

$[Au(edt^A)(edt^B)]^·$	1.34 eV
$[Au(edt^A)_2]^·$	0.79 eV
$[Au(edt^B)_2]^·$	0.69 eV

Fig. S9 DFT results for a model [Au(edt^A) (edt^B)] complex where the C=C bond lengths at the two sides have been shortened (1.240: edt^A)/lengthened (1.480: edt^B) to simulate the situation in asymmetric Au bis(dithiolene) complexes.

Table S3 C=C distances (Å) and spin location (%) for a model [Au(edt^{A}) (edt^{B})]$^{\bullet}$ complex where the C=C bond lengths at the two sides have been shortened /lengthened to simulate the situation in asymmetric Au bis(dithiolene) complexes.

r_A (Å)	r_B (Å)	$r_A - r_B$ (Å)	Spin A (%)	Spin B (%)
1.240	1.480	-0.240	9.2	90.8
1.280	1.440	-0.160	13.8	86.2
1.320	1.400	-0.080	23.6	76.4
1.357	1.357	+0.000	50.0	50.0
1.400	1.320	+0.080	76.4	23.6
1.440	1.280	+0.160	86.2	13.8
1.480	1.240	+0.240	90.8	9.2

Table S4. C=C distances (Å) and electron distribution (%) in a given spin-orbital for a model [Au(edt^{A}) (edt^{B})]$^{\bullet}$ complex where the C=C bond lengths at the two sides have been shortened /lengthened to simulate the situation in asymmetric Au bis(dithiolene) complexes. To facilitate the comparison with the real complexes we have kept the labeling SOMO, α SOMO−1, β SOMO−1, LUMO although in this model the β SOMO−1 is actually the highest occupied level.

r_A	r_B	SOMO (α)		SOMO-1 (α)		LUMO (β)		SOMO-1 (β)	
		A	B	A	B	A	B	A	B
1.240	1.480	73.9	26.1	26	74	11.6	88.4	88.1	11.9
1.280	1.440	77.9	22.1	22.5	77.5	16.1	83.9	84.5	15.5
1.320	1.400	76.1	23.9	22.6	77.4	24.7	75.3	73.8	26.2
1.357	1.357	50	50	50	50	50	50	50	50
1.400	1.320	23.9	76.1	77.4	22.6	75.3	24.7	26.2	73.8
1.440	1.280	22.1	77.9	77.5	22.5	83.9	16.1	15.5	84.5
1.480	1.240	26.1	73.9	74	26	88.4	11.6	11.9	88.1

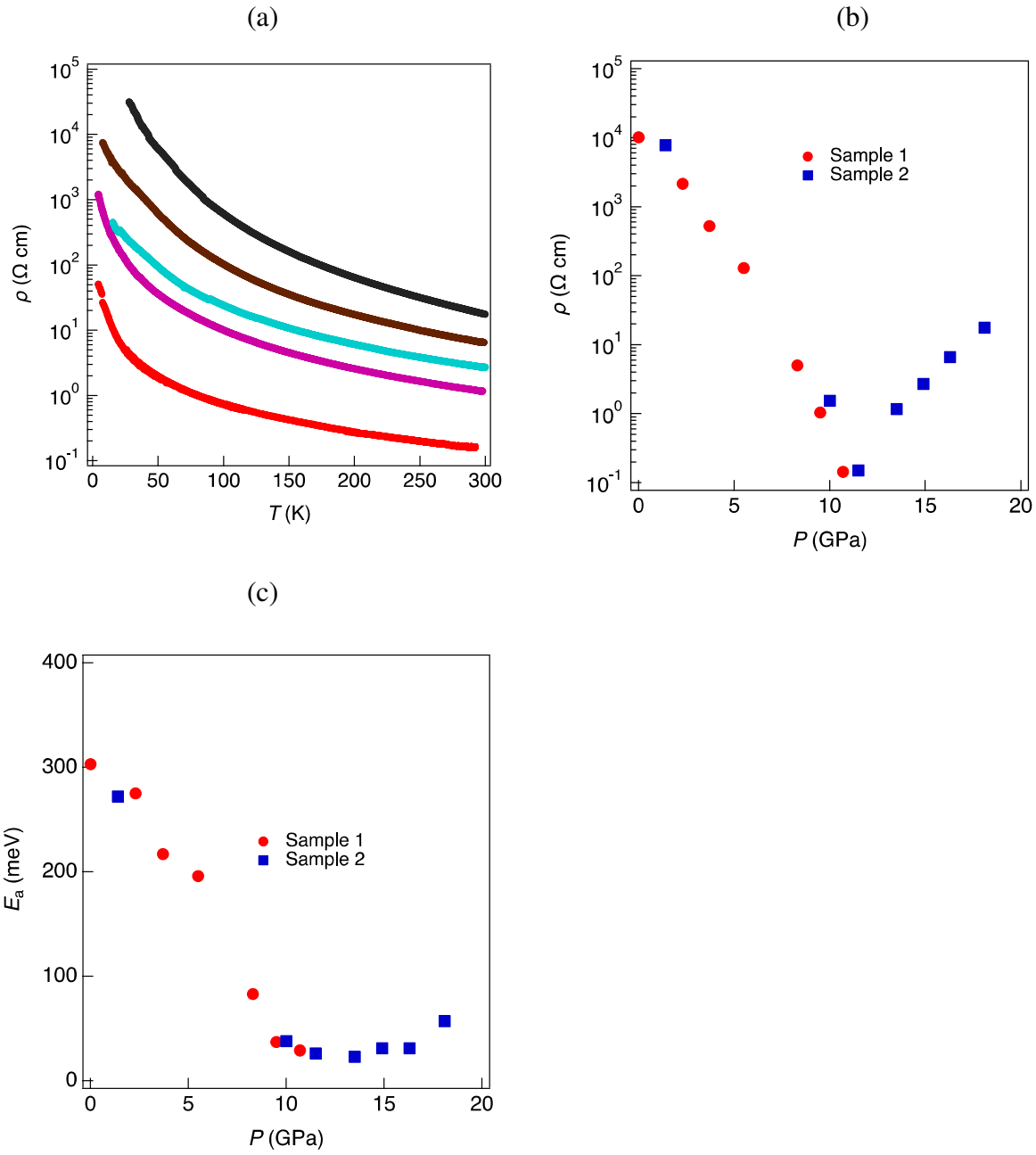

Fig. S10 (a) Temperature and pressure dependence of the resistivity of **1'** between 11.5 and 18.1 GPa. (b) Pressure dependence of the RT resistivity of **1'** between 1 bar and 18.1 GPa. (c) Pressure dependence of the activation energy of the resistivity of **1'** between 1bar and 18.1 GPa.

Table S5 Crystallographic data[a,b]

	$[Bu_4N][(pzdt)AuCl_2]$ **6**	$[Bu_4N][Au(bdt)_2]$
CCDC	2348567	2348571
Formulae	$C_{20}H_{38}AuCl_2N_3S_2$	$C_{28}H_{44}AuNS_4$
FW ($g.mol^{-1}$)	652.52	719.85
System	triclinic	orthorhombic
Space group	P−1	$Pna2_1$
a (Å)	9.1681(2)	16.4609(17)
b (Å)	10.7295(4)	19.7757(18)
c (Å)	13.7336(5)	18.6188(19)
α (deg)	88.3780(10)	90.00
β (deg)	77.4540(10)	90.00
γ (deg)	74.9480(10)	90.00
V ($Å^3$)	1272.89(7)	6060.9(10)
T (K)	150(2)	150(2)
Z	2	8
Cryst. dim. (mm)	0.43×0.29×0.11	0.12×0.08×0.06
D_{calc} ($g.cm^{-3}$)	1.702	1.578
μ (mm^{-1})	6.164	5.147
Absorption corr.	multi-scan	multi-scan
T_{min}, T_{max}	0.219, 0.508	0.657, 0.734
Total refls	14660	68653
Uniq refls (R_{int})	5742 (0.0397)	13902 (0.0339)
Uniq refls ($I > 2\sigma(I)$)	5494	13308
R_1, wR_2	0.0220, 0.0559	0.0162, 0.0388
R_1, wR_2 (all data)	0.0234, 0.0568	0.0187, 0.0402
GOF	1.018	0.872

[a] $R_1 = ||F_o| - |F_c||/|F_o|$. [b] $wR_2 = [w(F_o^2 - F_c^2)^2]/[w(F_{o2})^2]^{1/2}$.

Table S5 (continued). Crystallographic data[a,b]

	[Bu_4N] [Au(bdt)(Et-thiazdt)] **1**	[Bu_4N] [Au(pzdt)(Et-thiazdt)] **2**	[Au(bdt)(Et-thiazdt)] **1'**
CCDC	2348568	2348570	2348569
Formulae	$C_{27}H_{45}AuN_2S_6$	$C_{25}H_{43}AuN_4S_6$	C11 H9 Au N S6'
FW ($g.mol^{-1}$)	786.97	788.96	544.52
System	monoclinic	monoclinic	Triclinic
Space group	$P2_1/n$	$P2_1/c$	P−1
a (Å)	9.5242(11)	20.4897(19)	7.5222(6)
b (Å)	22.193(3)	12.2891(13)	7.5384(6)
c (Å)	16.2006(17)	26.698(2)	13.3073(13)
α (deg)	90.00	90.00	94.405(3)
β (deg)	105.821(4)	107.327(4)	97.176(3)
γ (deg)	90.00	90.00	94.089(3)
V ($Å^3$)	3294.6(7)	6417.4(11)	743.97(11)
T (K)	150(2)	150(2)	150(2)
Z	4	8	2
Cryst dim. (mm)	0.07×0.06×0.04	0.09×0.06×0.035	0.12×0.10×0.03
D_{calc} ($g.cm^{-3}$)	1.587	1.633	2.431
μ (mm^{-1})	4.865	4.997	10.711
Abst. corr.	multi-scan	multi-scan	multi-scan
T_{min}, T_{max}	0.710, 0.823	0.744, 0.840	0.493,0.725
Total refls	25969	98440	8615
Uniq refls (R_{int})	7559 (0.0483)	14669 (0.0415)	3356 (0.0254)
Uniq refls ($I > 2\sigma(I)$)	5912	12559	3217
R_1, wR_2	0.0451, 0.1311	0.0238, 0.0494	0.0187, 0.0460
R_1, wR_2 (all data)	0.0639, 0.1463	0.0318, 0.0519	0.0198, 0.0467
GOF	1.005	1.050	0.910

References

[1] N. Tenn, N. Bellec, O. Jeannin, L. Piekara-Sady, P. Auban-Senzier, J. Íñiguez, E. Canadell and D. Lorcy, A Single-Component Molecular Metal Based on a Thiazole Dithiolate Gold Complex, *J. Am. Chem. Soc*., 2009, **131**, 16961−16967

[2] Y. Le Gal, D. Ameline, N. Bellec, A. Vacher, T. Roisnel, V. Dorcet, O. Jeannin and D. Lorcy, Efficient routes towards a series of 5,5'-bithiazolidinylidenes as π-electron acceptors, *Org. Biomol. Chem*., 2015, **13**, 8479−8486

[3] S. R. Kennedy, M. N. Kozar, H. P. Yennawar and B. J. Lear, Synthesis and characterization of the gold dithiolene monoanion, $(Bu_4N)[Au(pdt = 2,3\text{-pyrazinedithiol})_2]$, *Polyhedron*, 2016, **103**, 100–104.

[4] G. M. Sheldrick, SHELXT – Integrated space-group and crystal-structure determination, *Acta Crystallogr*., 2015, **A71**, 3–8.

[5] G. M. Sheldrick, Crystal structure refinement with SHELXL, *Acta Crystallogr*., 2015, **C71**, 3–8.

[6] (a) M. Kaupp, M. Renz, M. Parthey, M. Stolte, F. Würthner and C. Lambert, Computational and spectroscopic studies of organic mixed-valence compounds: where is the charge? *Phys. Chem. Chem. Phys*., 2011, **13**, 16973–16986; (b) M. Parthey and M. Kaupp, Quantum-chemical insights into mixed-valence systems: within and beyond the Robin–Day scheme, *Chem. Soc. Rev*., 2014, **43**, 5067–5088.

[7] T. H. Dunning Jr. and P. J. Hay, in *Modern Theoretical Chemistry*, Ed. H. F. Schaefer III, Vol. 3 (Plenum, New York, 1977) 1–28.

[8] P. Schwerdtfeger, M. Dolg, W. H. E. Schwarz, G. A. Bowmaker and P. D. W. Boyd, Relativistic effects in gold chemistry. 1. Diatomic gold compounds, *J. Chem. Phys.*, **1989**, **91**, 1762–1774.

[9] P. Hohenberg and W. Kohn, Inhomogeneous Electron Gas, *Phys. Rev.,* 1965*,* **136***,* B864–B871.

[10] W. Kohn and L. J. Sham, Self-Consistent Equations Including Exchange and Correlation Effects, *Phys. Rev.,* 1965, **140***,* A1133–A1138.

[11] (a) J. M. Soler, E. Artacho, J. D. Gale, A. García, J. Junquera, P. Ordejón and D. Sánchez-Portal, The SIESTA method for ab initio order-N materials simulation, *J. Phys.: Condens. Matter.,* 2002*,* **14***,* 2745–2779; (b) E. Artacho, E. Anglada, O. Diéguez, J. D. Gale, A. García, J. Junquera, R. D. Martin, P. Ordejón, M. A. Pruneda, D. Sánchez-Portal and J. M. Soler, The SIESTA method: developments and applicability, *J. Phys.: Condens. Matter*., 2008, **20**, 064208; (c) A. García, N. Papior, A. Akhtar, E. Artacho, V. Blum, E. Bosoni, P. Brandimarte, M. Brandbyge, J. I. Cerdá, F. Corsetti, R. Cuadrado, V. Dikan, J. Ferrer, J. D. Gale, P. García-Fernández, V. M. García-Suárez, V. M. García, G. Huhs, S. Illera, R. Korytar, P. Koval, I. Lebedeva, L. Lin, P. López-Tarifa, S. G. Mayo, S. Mohr, P. Ordejón, A. Postnikov, Y. Pouillon, M. A. Pruneda, R. Robles, D. Sánchez-Portal, J. M. Soler, R. Ullah, Wen-zhe Yu and J. Junquera, SIESTA: Recent developments and applications, *J. Chem. Phys*., 2020, **152**, 204108, (d) For more information on the SIESTA code visit: http://departments.icmab.es/leem/siesta/

[12] J. P. Perdew, K. Burke and M. Ernzerhof, Generalized Gradient Approximation Made Simple, *Phys. Rev. Lett.,* 1966, **77**, 3865−3868.

[13] S. L. Dudarev, G. A. Botton, S. Y. Savrasov, C. J. Humphreys and A. P. Sutton, Electron-energy-loss spectra and the structural stability of nickel oxide: An LSDA+U study, *Phys. Rev. B: Condens. Matter Mater. Phys*., 1998, **57**, 1505−1509.

[14] Y. Kiyota, I.-R. Jeon, O. Jeannin, M. Beau, T. Kawamoto, P. Alemany, E. Canadell, T. Mori and M. Fourmigué, Electronic engineering of a tetrathiafulvalene charge-transfer salt via reduced symmetry induced by combined substituents, *Phys. Chem. Chem. Phys*., 2019, **21**, 22639−22646.

[15] N. Troullier and J. L. Martins, Efficient Pseudopotentials for planewave calculations, *Phys. Rev. B,* 1991*,* **43***,* 1993−2006.

[16] L. Kleinman and D. M. Bylander, Efficacious Form for Model Pseudopotentials, *Phys. Rev. Lett.,* 1982, **48***,* 1425−1428.

[17] E. Artacho, D. Sánchez-Portal, P. Ordejón, A. García and J. M. Soler, Linear Scaling ab-initio Calculations for Large and Complex Systems, *Phys. Stat. Sol. (b),* 1999, **215**, 809−817.

[18] P. Alemany, M. Llunell and E. Canadell, Uniform linear chains of group 11 atoms: do they have a bias towards a Peierls distortion? *Theor. Chem. Acc*., 2009, **123**, 85−92.

[19] H. J. Monkhorst and J. D. Pack, Special points for Brillouin zone integrations, *Phys. Rev. B,* 1976, **13**, 5188−5192.

[20] M.-H. Whangbo and R. Hoffmann, The band structure of the tetracyanoplatinate chain, *J. Am. Chem. Soc.*, 1978, **100**, 6093−6098.

[21] J. H. Ammeter, H. B. Bürgi, J. Thibeault and R. Hoffmann, Counterintuitive orbital mixing in semiempirical and ab initio molecular orbital calculations, *J. Am. Chem. Soc*., 1978, **100**, 3686−3692.

[22] Y. Le Gal, H. Cui, P. Alemany, E. Canadell, R. Kato, T. Roisnel, V. Dorcet, M. Fourmigué and D. Lorcy, Mixed-valence gold bis(diselenolene) complex turning metallic under pressure, *J. Mater. Chem. C*, 2021, **9**, 12291−12302.

[23] H. Cui, J. S. Brooks, A. Kobayashi and H. Kobayashi, A Single-Component Molecular Superconductor, *J. Am. Chem. Soc.,* 2009, **131**, 6358−6359.

[24] S. R. Kennedy, M. N. Kozar, H. P. Yennawar and B. J. Lear, Synthesis and characterization of the gold dithiolene monoanion, (Bu_4N)[Au(pdt = 2,3-pyrazinedithiol$)_2$], *Polyhedron,* 2016, **103**, 100−104.

[25] N. Tenn, N. Bellec, O. Jeannin, L. Piekara-Sady, P. Auban-Senzier, J. Íñiguez, E. Canadell and D. Lorcy, A Single-Component Molecular Metal Based on a Thiazole Dithiolate Gold Complex, *J. Am. Chem. Soc*., 2009, **131**, 16961−16967.